On the Relation among Satellite-Observed Liquid Water Path, Cloud Droplet Number Concentration, and Cloud-Base Rain Rate and Its Implication to the Autoconversion Parameterization in Stratocumulus Clouds

YASUTAKA MURAKAMI,[a,b] CHRISTIAN D. KUMMEROW,[a] AND SUSAN C. VAN DEN HEEVER[a]

[a] *Department of Atmospheric Science, Colorado State University, Fort Collins, Colorado*
[b] *Numerical Prediction Division, Japan Meteorological Agency, Tokyo, Japan*

(Manuscript received 22 June 2020, in final form 26 May 2021)

ABSTRACT: Precipitation processes play a critical role in the longevity and spatial distribution of stratocumulus clouds through their interaction with the vertical profiles of humidity and temperature within the atmospheric boundary layer. One of the difficulties in understanding these processes is the limited amount of observational data. In this study, robust relations among liquid water path (LWP), cloud droplet number concentration (N_d), and cloud-base rain rate (R_{cb}) from three subtropical stratocumulus decks are obtained from A-Train satellite observations in order to obtain a broad perspective on warm rain processes. The cloud-base rain rate R_{cb} has a positive correlation with LWP/N_d, and the increase of R_{cb} becomes larger as LWP/N_d increases. However, the increase of R_{cb} with respect to LWP/N_d becomes more gradual in regions with larger N_d, which indicates the relation is moderated by N_d. These results are consistent with our theoretical understanding of warm rain processes and suggest that satellite observations are capable of elucidating the average manner of how precipitation processes are modulated by LWP and N_d. The sensitivity of the autoconversion rate to N_d is investigated by examining pixels with small LWP in which the accretion process is assumed to have little influence on R_{cb}. The upper limit of the dependency of autoconversion rate on N_d is assessed from the relation between R_{cb} and N_d, since the sensitivity is exaggerated by the accretion process, and was found to be a cloud droplet number concentration to the power of -1.44 ± 0.12.

KEYWORDS: Cloud microphysics; Satellite observations; Cloud parameterizations

1. Introduction

Stratocumulus clouds persistently cover a large area of the globe. They have a significant impact on the global radiation budget and hydrological cycle (Slingo 1990). Drizzle plays an important but complicated role in the formation and maintenance of stratocumulus clouds through its interaction with the vertical profiles of humidity and temperature within the atmospheric boundary layer and the associated phase changes of the cloud and rain hydrometers (Wood 2012).

Stratocumulus droplet number concentrations vary as a function of aerosol number concentration. Cloud droplet number concentrations increase with increasing number concentrations of aerosol particles that act as cloud condensation nuclei (CCN; Twomey 1959). Cloud droplet number concentrations are typically high near the coast and low in remote oceans, varying from more than 500 cm^{-3} in polluted maritime regions to 10 cm^{-3} in pristine environments (e.g., Wood 2012). The fact that coastal waters off the west coast of subtropical continents are persistently covered by stratocumulus clouds makes these regions an ideal test bed for studying cloud physical and dynamical processes of warm rain clouds.

Numerous observational and modeling studies have been used to investigate the relation between rain rate and cloud droplet number concentration in stratocumulus clouds from the viewpoint of the impact of the change in background aerosol on precipitation efficiency, spatial distribution, and lifetime of cloud systems via its ability to modulate cloud droplet number concentration (second aerosol indirect effect; Albrecht 1989). The effect of aerosols on the spatial distribution and longevity of stratocumulus clouds differs among studies, although most find that higher CCN suppress rainfall. For example, Wood (2005a) showed that cloud-base rain rate in stratocumulus clouds decreases with higher cloud droplet number concentrations by utilizing observational data collected by aircraft in situ measurements and ground-based remote sensing from seven different field campaigns. Leon et al. (2008) found similar trends from *CloudSat* observations. Various modeling studies, including those utilizing large-eddy-simulations (LES; e.g., Ackerman et al. 2003) and cloud-resolving model simulations (e.g., Wang et al. 2011), also suggest that cloud-base rain rates of stratocumulus clouds decrease with higher cloud droplet number concentration. Sensitivity of cloud-base rain rate R_{cb} to cloud droplet number concentration N_d has been also extensively investigated in the framework of precipitation susceptibility metrics [$S_0 = \partial \ln R_{cb}/\partial \ln N_d$; Feingold and Siebert 2009]. Some studies (e.g., Terai et al. 2012) found that S_0 decreases monotonically with increasing liquid water path (LWP), while other studies (e.g., Jiang et al. 2010) reported that S_0 initially increases with LWP until reaches its maximum and then decreases. In terms of relation among R_{cb}, LWP and N_d, many previous studies have also found that R_{cb} not only weakens with increasing N_d but also intensifies with increasing LWP or cloud thickness H. For stratocumulus clouds off the coast of Peru, Comstock et al. (2004) derived an empirical relation, $R_{cb} \propto (\mathrm{LWP}/N_d)^{1.75}$, from shipborne observations consisting of radar, pyranometer, and microwave radiometer data. VanZanten et al. (2005) proposed a slightly different

Corresponding author: Yasutaka Murakami, yasutaka.murakami@colostate.edu

DOI: 10.1175/JCLI-D-20-0473.1

relation, $R_{cb} \propto H^3/N_d$, from aircraft in situ observations off the coast of California. LES studies (e.g., Geoffroy et al. 2008; Wang and Feingold 2009) reproduced relations among R_{cb}, N_d, and LWP that were consistent with those proposed by observational studies (e.g., Comstock et al. 2004; VanZanten et al. 2005), suggesting that the empirical relations derived from observations have a physical basis.

Abel et al. (2010) investigated the relation between R_{cb} and LWP for stratocumulus clouds over the southeast Pacific, using the United Kingdom's Met Office Unified Model with a one-moment cloud scheme. They assumed that the empirical relation proposed by Comstock et al. (2004) should be reproduced by the model and found that the results of their simulation best fit the Comstock et al. (2004) relation when assuming $N_d = 63\,\text{cm}^{-3}$ in the empirical relation. However, the simulations were actually conducted by prescribing $N_d = 100\,\text{cm}^{-3}$. Since larger N_d should suppress the rain production, their results suggested that the autoconversion scheme of the Unified Model was producing rain too efficiently.

The relation among R_{cb}, N_d, and LWP provides useful information, not only for an enhanced theoretical understanding of the mechanisms of stratocumulus formation, but also for the parameterization of precipitation processes in numerical weather and climate models. There are two contrasting but complementary approaches to study warm rain processes based on the relation among R_{cb}, N_d, and LWP. One way is to investigate how these processes are modulated with different droplet size distributions by deploying simulations that explicitly treat small-scale phenomena such as turbulence and entrainment (e.g., Wang and Feingold 2009). The other is to examine these processes based on the relation among the macrophysical variables obtained from observations (e.g., Comstock et al. 2004). This approach cannot explicitly account for small-scale processes, but they are reflected in the observed macrophysical variables and the observed relation among R_{cb}, N_d, and LWP serves as a constraint of numerical simulation results (e.g., Abel et al. 2010). We take the latter approach in this study, and we do so because warm rain processes are parameterized as functions of macrophysical variables in the bulk microphysics schemes used in many numerical weather prediction and convection permitting models. The set of observations and the statistical relationship among these physically important variables constitutes a behavior that models need to reproduce.

In previous observational studies, the relations among R_{cb}, N_d, and LWP are derived based on relatively small amounts of data from limited field campaign domains, which make globally applicable inferences difficult to draw. This study aims to obtain statistically robust relations among R_{cb}, N_d, and LWP for three geographical regions with similar environments, namely, the northeast Pacific off the coast of California, the southeast Pacific off the coast of Peru, and the southeast Atlantic off the coast of Namibia, by utilizing spaceborne observation from the A-Train satellites. Sensitivity of both the autoconversion rates and cloud-base rain rates to the cloud droplet number concentration is also assessed.

The outline of this paper is as follows: The data and methodology used to estimate cloud parameters from A-Train satellite observations is described in section 2. Section 3 presents the relations obtained from satellite observations and compares them with those of previous studies. Intercomparisons among the three study regions are also presented. The implication of these statistical relations to help represent autoconversion rates in bulk microphysics schemes is discussed in section 4. Conclusions from this study are given in section 5.

2. Estimation of stratocumulus cloud parameters from A-Train observations

a. Satellite data

Satellite observations from *CloudSat*'s Cloud Profiling Radar (CPR) (Stephens et al. 2002), *CALIPSO*'s spaceborne lidar (Winker et al. 2009), and *Aqua's* Moderate Resolution Imaging Spectroradiometer (MODIS) (Parkinson 2003), all of which fly in the A-Train, are used for estimating the cloud parameters in this study. All of the data are matched up to *CloudSat* footprints. The horizontal and vertical resolutions of *CloudSat* observations are approximately 1.75 km and 240 m, respectively. Cloud-base geometrical height and rain rates are estimated from the radar reflectivity profile through the Geometrical Profiling (GEOPROF) 2B-GEOPROF product (Marchand et al. 2008) with the method described below. Cloud-top geometrical height and cloud layers are derived from the 2B-GEOPROF-lidar product (Mace and Zhang 2014), and cloud optical thickness and cloud effective radius are derived from the MOD06.1KM-AUX product, which is a subset of MODIS. This Collection 6 cloud product is matched to the closest *CloudSat* footprints. Temperature and pressure data from ECMWF-AUX product are used as auxiliary data. The ECMWF-AUX product is a set of state variable of the fifth-generation ECMWF reanalysis (ERA5) interpolated to each *CloudSat* bin.

b. Methodology

1) Analysis of stratocumulus clouds

Subtropical maritime warm stratocumulus clouds off the west coast of various continents are analyzed in this study. Data for three years from 2008 to 2010 are used for the analysis. Although A-Train satellites have afternoon and nighttime equator crossing times, only daytime observations (around 1330 local time) are analyzed in this study because visible reflectance from MODIS visible bands are needed to derive LWP and N_d.

In this study, stratocumulus clouds are defined as single-layer low-level clouds whose cloud-top height and temperature are below 3000 m and above 268 K, respectively. Stratocumulus clouds existing in the northeast Pacific, the southeast Pacific or the southeast Atlantic (Table 1) are analyzed. The definition of the study regions is adopted from a previous study on the climatology of stratocumulus clouds (Muhlbauer et al. 2014). Under the subsidence regimes of the subtropical highs, mid- and upper-level cloud development is typically suppressed. The analysis was limited to single-layer clouds so as to select typical environments for the development of subtropical stratocumulus clouds. The International Satellite Cloud Climatology Project

TABLE 1. Analyzed regions and their location.

Region	Domain
Northeast Pacific (NEP)	15°–35°N, 120°–140°W
Southeast Pacific (SEP)	10°–30°S, 75°–95°W
Southeast Atlantic (SEA)	10°–30°S, 10°W–10°E

(ISCCP; Rossow and Schiffer 1991) defines low clouds by cloud-top pressures of less than 680 hPa, or maximum cloud-top geometric heights of 3000 m corresponding to 680 hPa in pressure coordinates. Aiming to select only liquid-phase clouds, the minimum cloud-top temperature is set to 268 K based on the criteria used in a previous study focused on estimating cloud droplet number concentration of stratocumulus clouds (Bennartz and Rausch 2017).

Figure 1 shows the frequency of occurrence of low clouds observed by *CloudSat*/*CALIPSO*. Regions enclosed by the red lines denote the selected analysis domains of this study. Figure 1a demonstrates the occurrence of low clouds, including those that are overlapped by higher clouds, while Fig. 1b shows the occurrence of single-layer low clouds only. Figure 1c shows the occurrence of clouds that meet the definition of stratocumulus clouds in this study. The frequent occurrence of low clouds in the subtropical oceans off the west coast of continents, the focus of this study, as well as those in the midlatitude storm tracks, are clearly evident in this figure. Low clouds found in the former regions tend to be more single-layered compared to those in the latter regions. This difference is likely the result of the different large-scale environments driving these systems.

2) ESTIMATION OF LWP AND N_d

LWP and N_d are calculated from the optical depth and effective radius provided by the MODIS collection 6 cloud product (Platnick et al. 2017). In this study, following Grosvenor et al. (2018), satellite-derived LWP and cloud droplet number concentrations N_d are computed as

$$\mathrm{LWP} = \frac{5}{9}\rho_w \tau r_e, \quad \text{and} \tag{1}$$

$$N_d = \frac{\sqrt{5}}{2\pi k}\left(\frac{f_{\mathrm{ad}} c_w \tau}{Q_{\mathrm{ext}} \rho_w r_e^5}\right)^{1/2}, \tag{2}$$

where ρ_w (kg m^{-3}) is density of water, τ is unitless cloud optical thickness, f_{ad} is the unitless adiabaticity factor, c_w (kg m^{-4}) is adiabatic condensate rate, and $Q_{\mathrm{ext}} = 2$ is the unitless extinction efficiency factor. The variable k is defined in Eq. (3), which relates droplet effective radius r_e and volume-mean radius r_v (Hansen and Travis 1974) defined as Eqs. (4) and (5), respectively:

$$k = \left[\frac{r_v(z)}{r_e(z)}\right]^3, \tag{3}$$

$$r_e(z) = \frac{\int_0^\infty r^3 n(r)\, dr}{\int_0^\infty r^2 n(r)\, dr}, \quad \text{and} \tag{4}$$

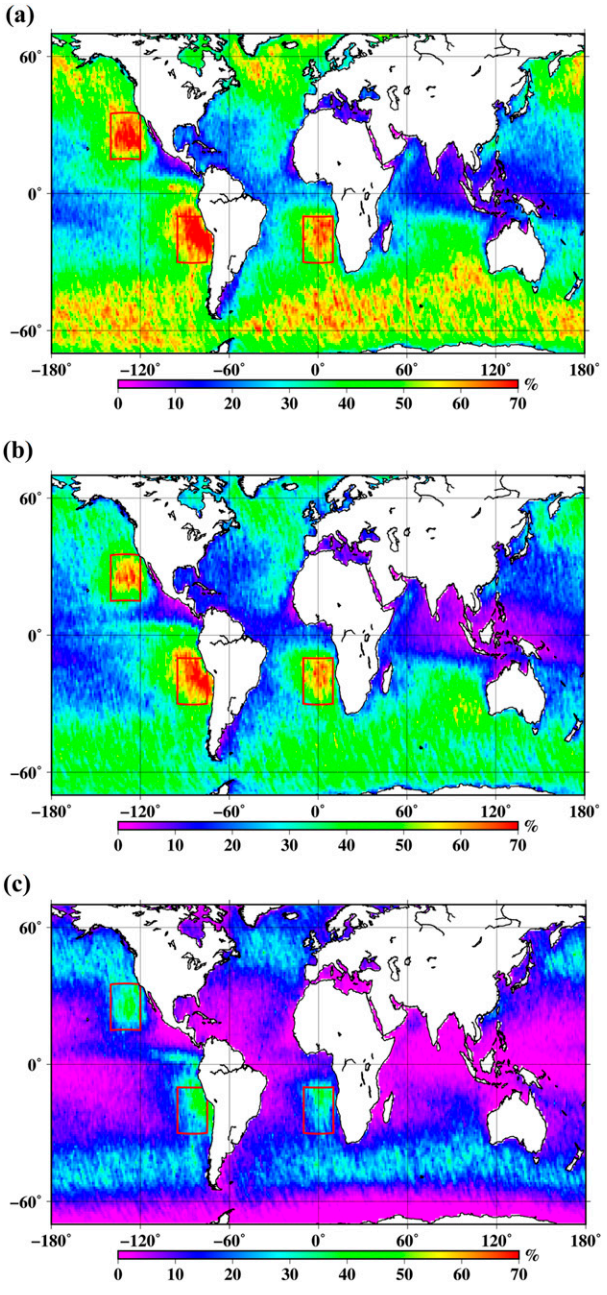

FIG. 1. Frequency of occurrence of low clouds observed by *CloudSat*/*CALIPSO* for (a) those overlapped by higher clouds, (b) single-layer low clouds only, and (c) clouds defined as stratocumulus clouds in this study (i.e., single-layer clouds whose cloud-top height and temperature are below 3000 m and above 268 K, respectively). Regions enclosed by the red rectangles indicate the analysis areas in this study. The data period is three years from 2008 to 2010, and observations are made at daytime (approximately 1330 local time). Grid resolution is 1°.

$$r_v^3(z) = \frac{1}{N_d(z)}\int_0^\infty r^3 n(r)\, dr. \tag{5}$$

Equations (1) and (2) are derived based on the assumptions that 1) stratocumulus clouds are horizontally homogeneous, 2)

cloud liquid water content (LWC) increases monotonically within the cloud layer, and 3) cloud droplet number concentrations are vertically constant within the cloud layer. Many in situ observation and modeling studies show that these assumptions are generally valid for stratocumulus clouds (e.g., Nicholls and Leighton 1986; Brenguier et al. 2000; Wood 2005a; Klein et al. 2009). Comparison studies (e.g., King and Vaughan 2012) between MODIS-derived and in situ LWP show that MODIS-derived LWP assuming monotonically increasing LWC is less biased than those assuming vertically constant LWC.

The MODIS cloud product provides effective radius estimates using observations from 1.6, 2.1, and 3.7 μm. Studies have suggested that estimates of the cloud effective radius from 3.7 μm ($r_{e,3.7}$) is less prone to pixel heterogeneity compared to the other two (Grosvenor et al. 2018) and is therefore used for this study. The adiabatic condensate rate c_w is calculated from the cloud-base pressure and temperature obtained from ECMWF-AUX product with the assumption that c_w is vertically constant within the cloud layer. Cloud base is determined using the *CloudSat* radar profile.

Based on the results of aircraft observations (Martin et al. 1994; Pawlowska and Brenguier 2003), the value of k is set to 0.8. Adiabaticity f_{ad} is set to 1, which follows previous studies for estimating cloud droplet number concentration from MODIS observations that assume condensation rates to be completely adiabatic (e.g., Bennartz 2007). Clouds are diabatic in nature and this will lead to overestimation of N_d. In situ observations from Second Dynamics and Chemistry of Marine Stratocumulus field study (DYCOMS II) show that it varies from 0.67 to 0.90 (Brenguier et al. 2011). However, its impact is considered to be relatively small because retrieved N_d is proportional to the square root of adiabaticity.

LWP and N_d are calculated only for those pixels whose optical thickness exceeds 5, and effective radius satisfies $r_{e,3.7} > r_{e,2.1} > r_{e,1.6}$. The former criterion is used to exclude thin clouds that typically have larger estimation errors for their effective radius due to their sensitivity to reflectance, while the latter criterion is for extracting relatively homogeneous pixels, which also satisfy our cloud assumption that liquid water content monotonically increases with height within the cloud layer. Screening out clouds with $\tau < 5$ is reducing the sample by approximately 24%.

3) CLOUD-BASE HEIGHT

Cloud base is defined from the vertical profile of the *CloudSat* radar reflectivity. Previous observational studies of stratocumulus have suggested that radar reflectivity reaches its maximum around cloud base (Wood 2005a; vanZanten et al. 2005). This is consistent with our theoretical understanding of warm rain precipitation processes in which rain embryos formed near the cloud top grow by collecting cloud droplets while falling through the cloud layer but decrease in size once below cloud base due to evaporation. Cloud base is defined as the radar bin that has the largest reflectivity among the bins between the fifth bin from the surface (i.e., 960 m from the surface) and cloud top identified in the 2B-GEOPROF-lidar product, after correcting for water vapor attenuation using the value provided in 2B-GEOPROF product. *CloudSat* operates at a frequency of 94 GHz, which is heavily affected by attenuation due to water vapor and hydrometeors. Only water vaper attenuation is considered for determining cloud base because vertical change of total attenuation by cloud droplets is much smaller than that by water vapor near cloud base.

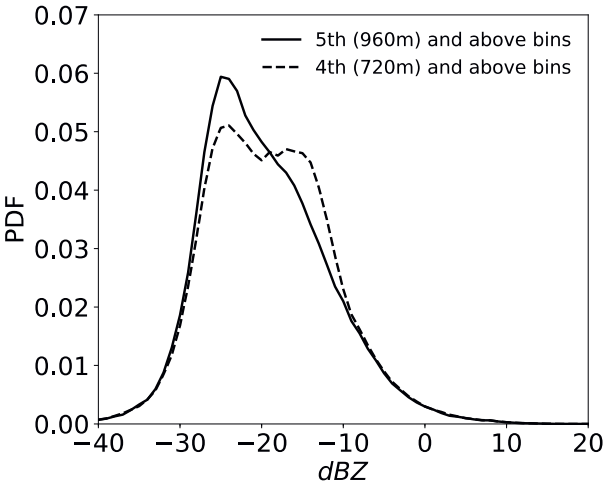

FIG. 2. Probability density distributions of estimated cloud-base radar reflectivity when utilizing the fifth bin and above (solid line) and the fourth bin and above (dashed line), respectively. The former adopts the same assumption as employed in this study.

Radar reflectivity data of the nearest four bins to the surface (i.e., below 960 m in altitude) are excluded from our analysis because these bins are heavily contaminated by surface clutter (Marchand et al. 2008). This treatment will lead to the overestimation of cloud-base height, especially in the case when the actual cloud base is below 1 km AGL. However, from the following physical consideration and observational results, we assume that the effect of this treatment on the estimated cloud-base radar reflectivity is small. From the cloud physics point of view, cloud droplet effective radius increases going upward within the cloud while drizzle drop sizes increase as they fall through the cloud to reach a maximum at cloud base and eventually decreases at subcloud layer due to evaporation. It can be assumed that raindrops, which are the dominant contributor to the increase of radar reflectivity, will grow slowly near cloud base since accretional growth is small due to small cloud liquid water content and small collection efficiency for cloud droplets in this region. In fact, previous studies using ground-based radar observation of stratocumulus clouds have found that the radar reflectivity increases rapidly near cloud top and remains fairly constant near cloud base (Comstock et al. 2004), which is in support of this assumption.

Figure 2 shows the probability density distributions of cloud-base radar reflectivity estimated from the algorithm used in this study and from a slightly different algorithm that includes an additional bin closer to the surface (the fourth bin from the surface). Overall, the probability density distributions are similar, which suggests that the effect of overestimating cloud-base height on the estimated cloud-base reflectivity is small. However, if the fourth bin from the surface is allowed in this

analysis, there is a peak around −15 dBZ that is not found when this bin is removed. Since the peak around −15 dBZ in Fig. 2 corresponds to the estimated surface clutter of *CloudSat* at the fourth bin from the surface (see Fig. 7 of Marchand et al. 2008), it would appear that using this bin in the current study would heavily affect the estimated cloud-base radar reflectivity. The fourth bin is therefore excluded from this analysis.

4) Estimation of R_{cb}

The precipitation of stratocumulus clouds is generally weak and thus the evaporation of raindrops in the subcloud layer is not negligible. Since our interest is in the precipitation formation of stratocumulus clouds, we focus specifically on the rain rate at cloud base, which is considered to be the strongest rate within the column. A reflectivity to rain rate (Z–R) relation is employed to estimate R_{cb} from the radar reflectivity observed by *CloudSat*. To account for uncertainties in rain/drizzle/cloud droplet size distributions of stratocumulus clouds (e.g., Table 1 of Miles et al. 2000), rain rate is calculated as the mean of those derived from five different Z–R relations presented in previous aircraft and ground-based observational studies. Maximum and minimum values obtained from the five different Z–R relations are used to define an estimation error. Figure 3 shows the Z–R relations employed in this study, as well as the five relations presented in the previous studies. The analyzed regions and observation methods, as well as parameters of five Z–R relations used in this study are provided in Table 2. These relations were obtained from ground-based radar and aircraft observations of southeast Pacific stratocumulus clouds from the East Pacific Investigation of Climate (EPIC) field campaign (Comstock et al. 2004) and aircraft observations of northeast Atlantic stratocumulus clouds (Wood 2005b). We expect that the inclusion of the Z–R relations derived in the northeast Atlantic, which is outside of our interest in this study, will incorporate a wide range in the droplet size distributions due to their different environments outside of subtropical subsidence regions. To account for the disproportionate impact of large drops that in situ aircraft observations often underestimate, we employ two types of Z–R relations derived from aircraft observation. The first uses an extrapolated droplet size distribution assuming an exponential shape and the second is without extrapolation.

The Z–R relations are applied to radar reflectivity data corrected for water vapor and cloud droplet attenuation and temperature dependency of the index of refraction. The correction for water vapor attenuation is employed from the 2B-GEOPROF product that is the same as that used for determining cloud-base height. Equation (6), which was proposed by Liebe et al. (1989), is used to correct for cloud droplet attenuation:

$$\alpha = La\theta^b. \tag{6}$$

Here, α is the cloud droplet attenuation (dB km^{-1}), L is the LWC (g m^{-3}), θ is defined as $\theta = 300/T_{cb}$ where T_{cb} (K) is cloud-base air temperature, $a = 3.73$, and $b = 2.81$. It is worth noting that Eq. (6) was found to be valid for airborne W-band radar observation of stratocumulus clouds (Vali and Haimov 2001).

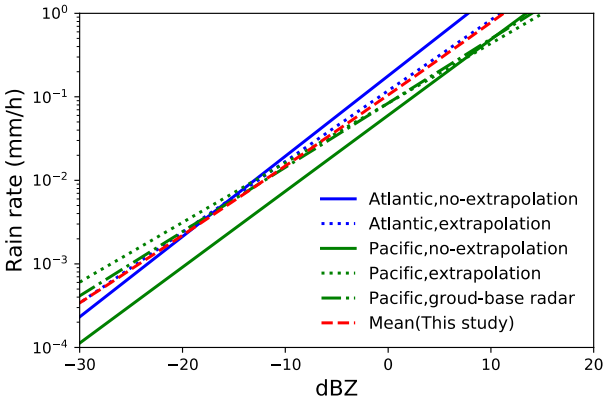

FIG. 3. The Z–R relation employed in this study and those from five previous studies. Atlantic and Pacific Z–R relations are obtained from aircraft observation of northeast Atlantic stratocumulus clouds (Wood 2005b) and ground-based radar and aircraft observation of southeast Pacific stratocumulus clouds from the EPIC field campaign (Comstock et al. 2004), respectively.

These Z–R relations are applied for reflectivities between −25 and 10 dBZ, corresponding to the range for which they were originally derived. Uncertainties due to the difference in Z–R relations are also assigned to this range. For those data outside of this range, it is assumed that the estimated rain rate is only qualitatively valid and estimation uncertainties are not evaluated.

c. *Characteristics of analyzed clouds*

The characteristics of estimated R_{cb}, N_d, and LWP for Californian [northeast Pacific (NEP)], Peruvian [southeast Pacific (SEP)], and Namibian [southeast Atlantic (SEA)] stratocumulus clouds are explored. Cloud-top height serves as a good indicator for the thickness of the atmospheric boundary layer in these three regions since they are determined mainly by the strength of the subsidence flow from the subtropical high, and hence by the corresponding inversion layer. Figure 4 shows probability density functions of cloud-top height, N_d, LWP, and cloud-base radar reflectivity of the data that pass the quality control procedure described in this section. The peak of the cloud-top height is located at around 1500 m for all three regions (Fig. 4a), which is consistent with the result of Takahashi et al. (2017). We therefore assume that there is no significant difference among analyzed clouds from the three different regions in terms of their dynamical and thermodynamical environment. It is also noted that clouds with top heights of less than 1000 m are not analyzed in this study by design.

LWP is distributed broadly from less than 20 g m^{-2} to more than 300 g m^{-2} with a mode located around 70 g m^{-2} for all three regions (Fig. 4c). NEP has a tendency for larger LWP compared to the other two regions. The cloud droplet number concentration N_d (Fig. 4b) is also broadly distributed and ranges from less than 10 cm^{-3} to more than 300 cm^{-3} for all three regions. The distribution of cloud-base radar reflectivity (Fig. 4d) is nearly the same for all three regions. The majority

TABLE 2. Analyzed region, observation method, and derived Z–R relations in previous studies (Wood 2005b; Comstock et al. 2004); a and b are parameters defining the Z–R relation where $Z = aR^b$.

Region	Observation method	a	b
Northeast Atlantic (Wood 2005b)	Aircraft (with extrapolation)	6.0	1.04
	Aircraft (without extrapolation)	12.4	1.18
Southeast Pacific (Comstock et al. 2004)	Aircraft (with extrapolation)	22	1.1
	Aircraft (without extrapolation)	32	1.4
	Ground-based radar	25	1.3

of the observations have radar reflectivity of less than −20 dBZ, suggesting light- or nonprecipitating clouds. Heavily precipitating clouds with radar reflectivity exceeding 10 dBZ are not present in these three analysis domains, which is in keeping with our theoretical expectations of stratocumulus precipitation rates.

3. Result

a. Determining factors of warm rain cloud-base rain rate

Precipitation particles observed at the base of a warm cloud are formed through conversion of cloud droplets to raindrop embryos (autoconversion), followed by growth of those rain embryos through the collection of cloud droplets as they fall through the cloud layer (accretion). While both of them represent the collision–coalescence of hydrometers with different size, we will distinguish these two in our discussion following common usage. Since these processes are modulated by N_d and LWP, the relation between these parameters and R_{cb} contains information on autoconversion and accretion. As we are only analyzing those stratocumulus clouds developing in similar environments, it is assumed that the following two approximations are valid. First, condensate rate of the analyzed clouds can be approximated as the same because they exist in similar environments. Combining this approximation with the observational fact that LWC monotonically increase within the cloud layer (e.g., Wood 2005a), we can assume that cloud-top LWC, which is one of the main two controlling factor of autoconversion, is a function of LWP. The second is that the average vertical motion of the analyzed clouds are similar because they exist in similar

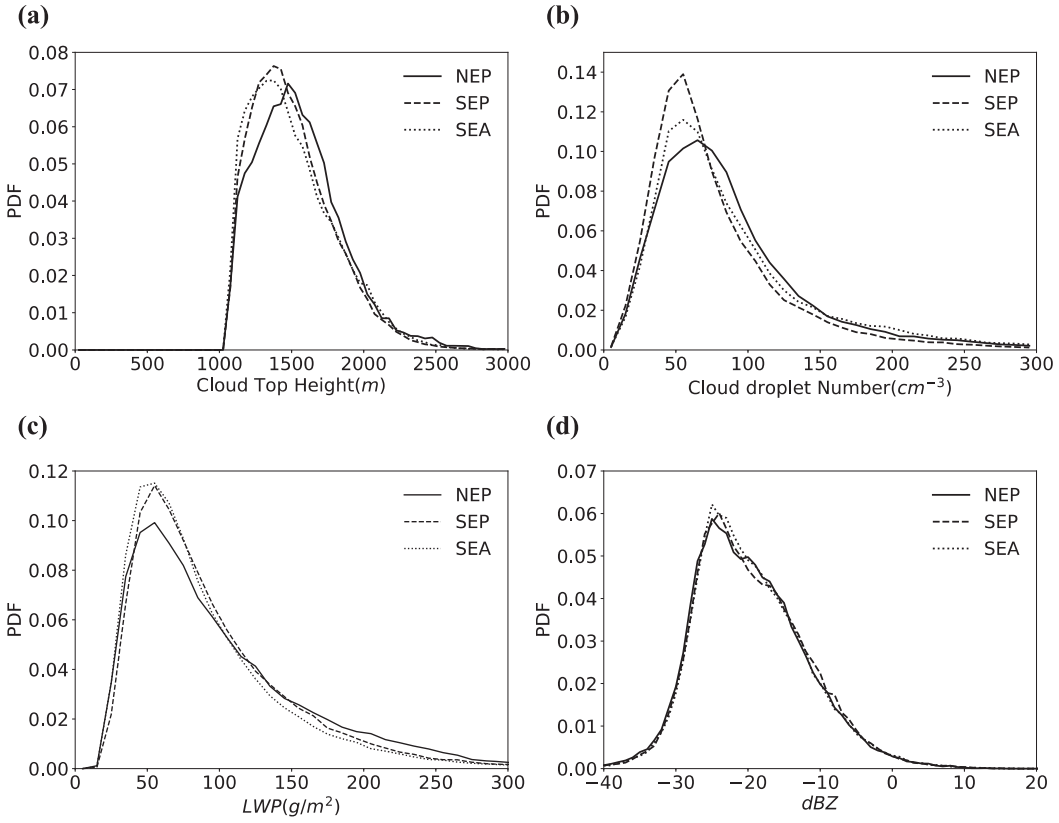

FIG. 4. Probability density functions of (a) cloud-top height, (b) cloud droplet number concentration, (c) LWP, and (d) cloud-base radar reflectivity for NEP (Solid lines), SEP (dotted lines) and SEA (dashed lines).

environments. Considering the growth of rain droplets within the continuous growth framework (e.g., Rogers and Yau 1989), raindrops from clouds with similar LWP will sweep out similar amounts of liquid water until they reach cloud base. Based on these approximations, we qualitatively discuss the impact of autoconversion related to N_d and LWP. It should be noted that other factors that vary with environment, such as turbulent mixing, also play role in autoconversion. While those effects should be also explored further, we will focus on the impact of N_d and LWP as a first-order approximation in this study.

The autoconversion rate P is determined by the size distribution and collision–coalescence efficiency of cloud droplets. Many model parameterizations have been proposed with different assumptions regarding the cloud droplet size distributions (e.g., Berry and Reinhardt 1974; Khairoutdinov and Kogan 2000). These schemes can be expressed by the following general formula, where $H(y - y_c)$ is the Heaviside step function:

$$P \propto \mathrm{LWC}^{\alpha} N_d^{-\beta} H(y - y_c). \tag{7}$$

Typically, y and y_c are both function of cloud droplet sizes, where y is related to the mean cloud droplet size and y_c is related to its threshold. Equation (7) implies that cloud droplets should be larger than a certain size for the activation of autoconversion. It also implies that at a given N_d, higher LWC (LWP) near cloud top will promote the conversion of cloud droplets to raindrop embryos by enhanced collision–coalescence efficiency due to larger cloud droplet sizes, whereas higher N_d will suppress the autoconversion, by effectively reducing cloud droplet sizes and hence the collision–coalescence efficiencies.

Raindrop embryos produced by autoconversion will grow and eventually become raindrops by collecting cloud droplets while they fall through the cloud layer. In continuous collection model, growth of raindrops between cloud top and bottom (dr_d) can be written as a product of cloud-layer-mean collection efficiency of cloud droplets by rain [$\overline{K(r_d, r_c)}$] and LWP (i.e., dr_d increases as $\overline{K(r_d, r_c)}$LWP increases). Collection efficiency generally has a higher efficiency for larger cloud droplets. Since cloud droplet size tends to be larger for larger LWC (LWP) and fewer N_d as a first-order approximation, the growth rate of raindrops becomes larger with fewer N_d and larger LWP in this simple growth model framework.

Enhanced raindrop embryo production near the cloud top and efficient accretional growth of raindrop within the cloud layer will intensify the cloud-base rain rate R_{cb}. Since both of them increase with larger LWP and fewer N_d, R_{cb} will be intensified by increasing LWP and decreasing N_d. Therefore, if a numerical model tends to simulate stronger (weaker) R_{cb} compared to the observation of clouds with the same N_d and LWP, we could infer that the model representation of autoconversion or accretion growth is overestimated (underestimated).

As summarized in Geoffroy et al. (2008), a number of empirical formulae have been proposed from different observations for the relation among R_{cb}, N_d, and LWP. These include $R_{\mathrm{cb}} \propto \mathrm{LWP}^2/N_d$ from the second Aerosol Characterization Experiment (ACE-2) (Raes et al. 2000), $R_{\mathrm{cb}} \propto (\mathrm{LWP}/N_d)^{1.75}$ from EPIC (Bretherton et al. 2004), and $R_{\mathrm{cb}} \propto \mathrm{LWP}^{1.5}/N_d$ from DYCOMS II (Stevens et al. 2003). In this study, we employed the empirical relation obtained from the EPIC field campaign $R_{\mathrm{cb}} \propto (\mathrm{LWP}/N_d)^{1.75}$ (Comstock et al. 2004) as a baseline.

b. R_{cb} as a function of N_d/LWP

Figure 5 shows the probability density distribution of R_{cb} as a function of the ratio of LWP to N_d (LWP/N_d) for the three regions investigated here. All three probability density distributions have similar patterns, thus suggesting that drizzle formation processes of stratocumulus clouds in these subtropical subsidence flow regions are largely the same. The cloud-base rain rate R_{cb} has a positive correlation with LWP/N_d and the increase of rain rate becomes larger as LWP/N_d becomes larger, which is consistent with our physical understanding that larger cloud droplets near cloud top will enhance the raindrop embryo production through autoconversion and subsequent accretion growth of raindrops. Larger LWP/N_d implies larger cloud-top droplet size because cloud-top LWC has a positive correlation with LWP that is drawn from our assumption that LWC increases with geometrical height within the cloud layer with similar condensate rates. In the region of LWP/N_d less than 1, the increase of R_{cb} with respect to LWP/N_d becomes more gradual. This is also consistent with our physical understanding that cloud droplets need to be larger than a certain size for autoconversion to be enhanced. Although the slope of R_{cb} with respect to LWP/N_d is nearly the same as the results of Comstock et al. (2004) in the region of LWP/N_d greater than 1, the absolute value of R_{cb} in this study is one order of magnitude smaller than that of Comstock et al. (2004). Since similar Z–R relations are employed to estimate R_{cb} from radar reflectivity in both studies, this is unlikely to have a large impact on the rain rate. It is more likely that the difference between these two studies comes from the overestimation of LWP/N_d. It is possible that either the LWP is overestimated and/or N_d is underestimated in this study, which result in the overestimation of LWP/N_d.

We consider such over and underestimations of LWP and/or N_d are due to the following two reasons. First, the physical meaning of the estimated N_d is different between these two studies. Comstock et al. (2004) employed cloud optical thickness and LWP obtained from a ground-based pyranometer and microwave radiometer to compute the cloud layer mean N_d. In this study, we estimate the near-cloud-top value using MODIS effective radius and cloud optical thickness. Although N_d is assumed to be vertically constant in estimating N_d from MODIS products, strictly speaking, it is not vertically constant in nature. The cloud droplet concentration N_d tends to decrease as the altitude increases (e.g., Painemal and Zuidema 2011) due to the collision–coalescence between cloud droplets, the expansion of air parcels and the evaporation caused by entrainment, Thus, satellite-derived N_d are often smaller than those derived from ground-based observation.

Second, a positive bias of MODIS cloud droplet radius leads to an overestimation of LWP and an underestimation of N_d, both of which result in the overestimation of LWP/N_d [see Eqs. (1) and (2)]. Noble and Hudson (2015) found that the effective radius derived from MODIS 2.1-μm channel is larger than

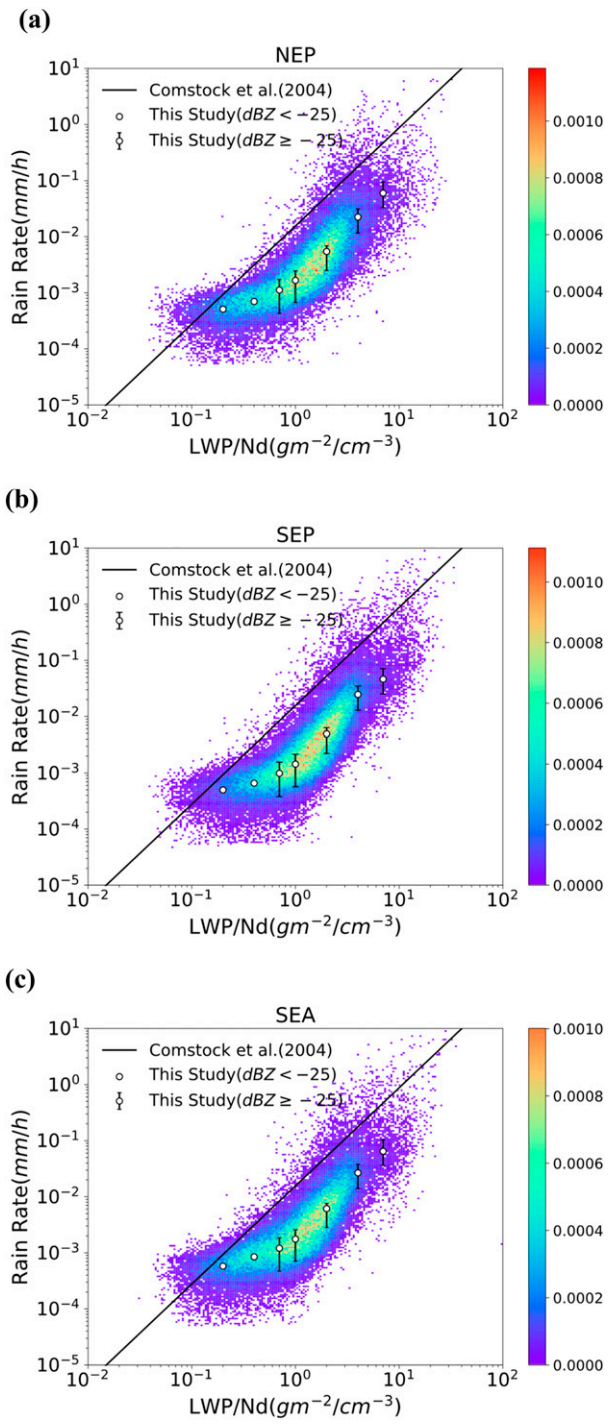

FIG. 5. Probability density distributions of cloud-base rain rate and the ratio of LWP to N_d (LWP/N_d) for (a) NEP, (b) SEP, and (c) SEA. White circles denote median cloud-base rain rate. The relation presented in Comstock et al. (2004) is denoted in solid black lines.

aircraft in situ measurement of cloud droplet size at cloud top by 20%–30% for northeast Pacific stratocumulus clouds. Since we are only analyzing those data satisfying $r_{e,3.7} > r_{e,2.1} > r_{e,1.6}$, the bias could be even more pronounced. Figure 6 shows the probability density distributions of R_{cb} and LWP/N_d after adjusting the LWP/N_d by −70% [i.e., $(\text{LWP}/N_d)_{\text{calibrated}} = (\text{LWP}/N_d)_{\text{MODIS}}/3.35$]. The adjustment factor of −70% is derived by assuming overestimation of MODIS $r_{e,3.7}$ of 25% and the cloud droplet number concentration at cloud top of 65% of that of the cloud layer mean. In the region where LWP/N_d is greater than 0.3, the probability density distributions from the three regions are now much more similar to those of Comstock et al. (2004). In the following figures, we do not apply the adjustment factor as it was used only to compare the two above estimates.

Figure 7 shows R_{cb} as a function of the ratio of LWP to N_d (LWP/N_d) for various ranges of N_d. All three regions show similar patterns of high (low) N_d being located in the region of small (large) LWP/N_d ratios. The R_{cb} and its change for points with high N_d are smaller compared to those with lower N_d, suggesting that the relation between R_{cb} and LWP can be differentiated by N_d. It is important to sort the data by N_d when discussing the dependency of R_{cb} on LWP and N_d. This observational result also suggests that the dependency of R_{cb} on N_d become stronger with increasing LWP, which is consistent with the previous modeling study (Feingold et al. 2013).

The value of γ and δ in $R_{cb} \sim \text{LWP}^{\gamma} N_d^{\delta}$ relationship is examined from the satellite data utilized in this study. The value of γ is evaluated to be 1.74, 1.77, and 1.80, and δ is −0.79, −1.06, and −0.80 for NEP, SEP, and SEA, respectively. These values are within the range of previous studies that vary from 1.5 (Kostinski 2008) to 2 (Geoffroy et al. 2008) for γ and from −1/3 (Wang and Feingold 2009) to −1.75 (Comstock et al. 2004) for δ.

c. *Response of R_{cb} to N_d and LWP*

Figure 8 shows that R_{cb} decreases with higher N_d regardless of LWP, which demonstrates more clearly that higher N_d suppress the raindrop growth. It should be also noted that the dependency of R_{cb} on N_d and LWP varies with LWP and N_d, respectively, which could be one of the reasons why previous studies resulted in similar but slightly different relations on these variables. To further illuminate the varying response of R_{cb} to N_d and LWP with respect to N_d and LWP, R_{cb} is plotted in LWP–N_d space (Fig. 9). Clouds with relatively heavy drizzle (>0.1 mm h^{-1}) have lager variability in LWP for a given N_d, which is consistent with the finding of modeling study by Nelson et al. (2016). Nondrizzling or light drizzle clouds (<0.001 mm h^{-1}) tend to have higher N_d compared to heavily drizzling cloud.

4. Discussion

a. *Accretion effect on rain rate sensitivity to N_d*

The results presented in the previous section clearly show that the varying response of R_{cb} to N_d and LWP. In this section, this varying response and its relation to autoconversion and accretion is discussed. Figure 10 shows the cloud-top (left panels) and cloud-base (right panels) rain rate as a function of N_d for different cloud-top LWCs. The same Z–R relation is employed for the rain rate calculation at both cloud top and cloud base. Here, we assume that a Z–R relation, which is derived from cloud-base and/or cloud-layer-mean droplet size

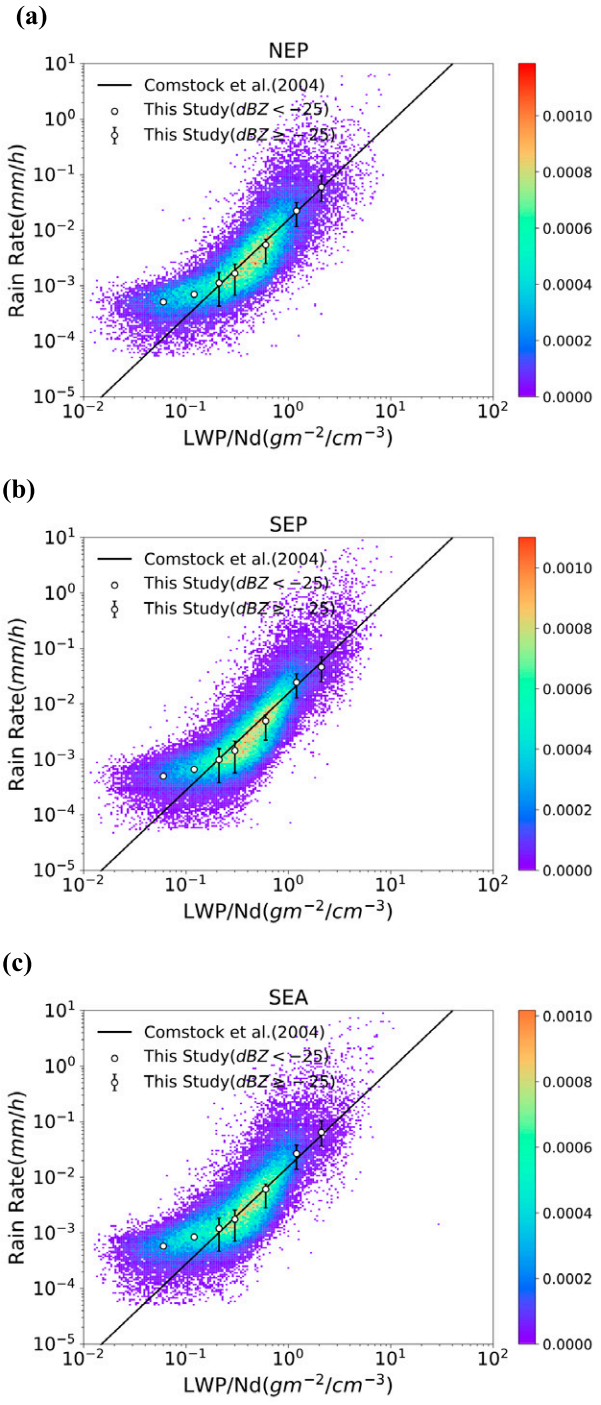

FIG. 6. As in Fig. 5, but after correcting for the different definition of N_d and potential differences arising from the MODIS cloud droplet biases.

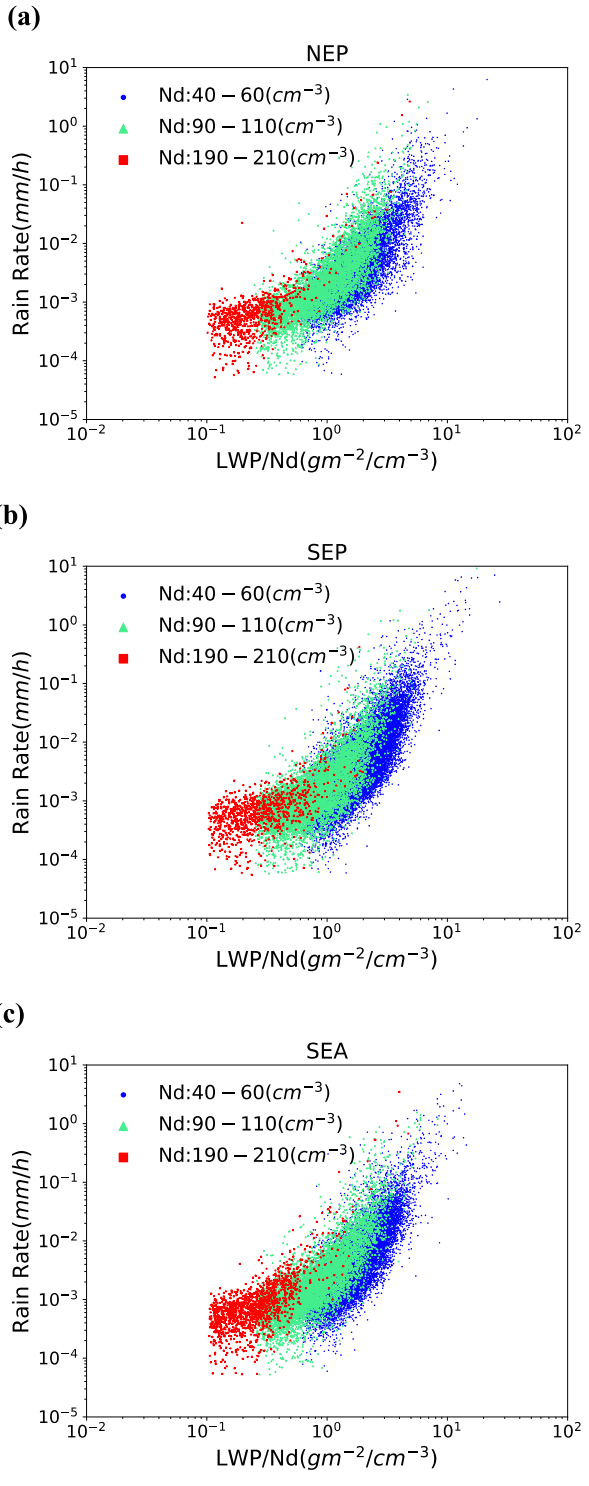

FIG. 7. Cloud-base rain rate as a function of the ratio of LWP to N_d (LWP/N_d) for (a) NEP, (b) SEP, and (c) SEA. Data are classified by cloud droplet number concentration; 40–60 cm^{-3} (blue dot), 90–110 cm^{-3} (green triangle), and 190–210 cm^{-3} (red rectangle).

distributions, is applicable to estimate cloud-top rain rates within acceptable errors. As shown by Wood (2005b), the difference in droplet size distributions between cloud top and cloud base is unlikely to affect the validity of using the *Z–R* relation in shallow stratocumulus clouds. Cloud-top liquid

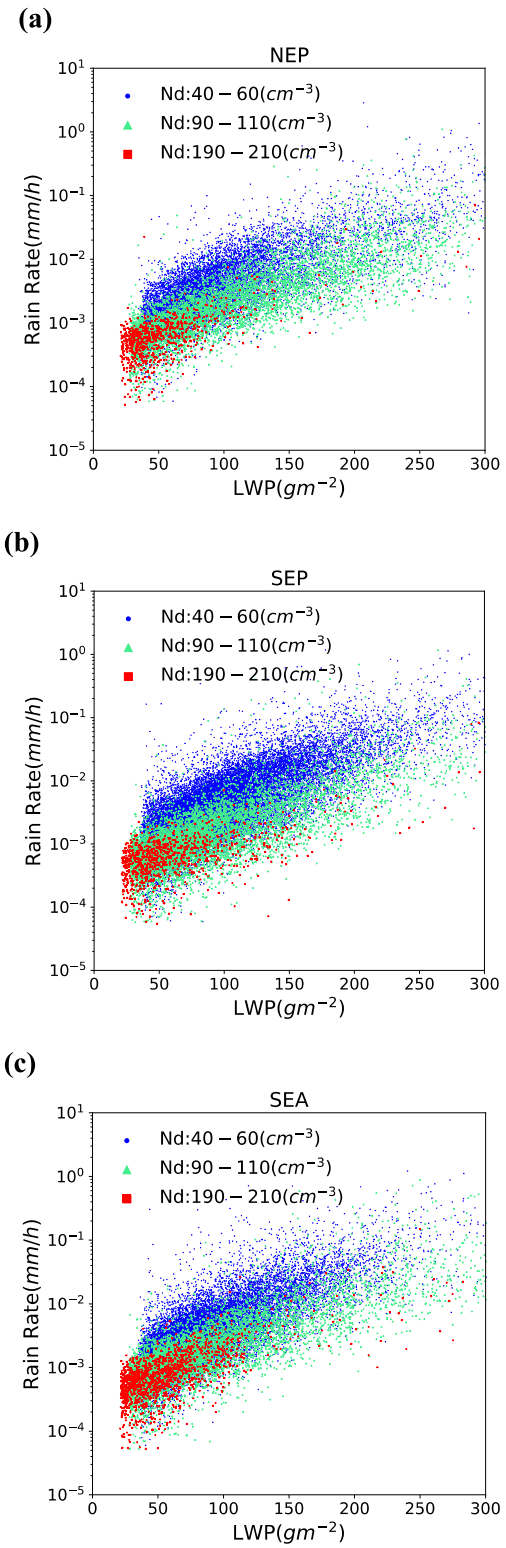

FIG. 8. Cloud-base rain rate as a function of LWP for (a) NEP, (b) SEP, and (c) SEA. Notations of cloud droplet number concentration range are same as Fig. 7.

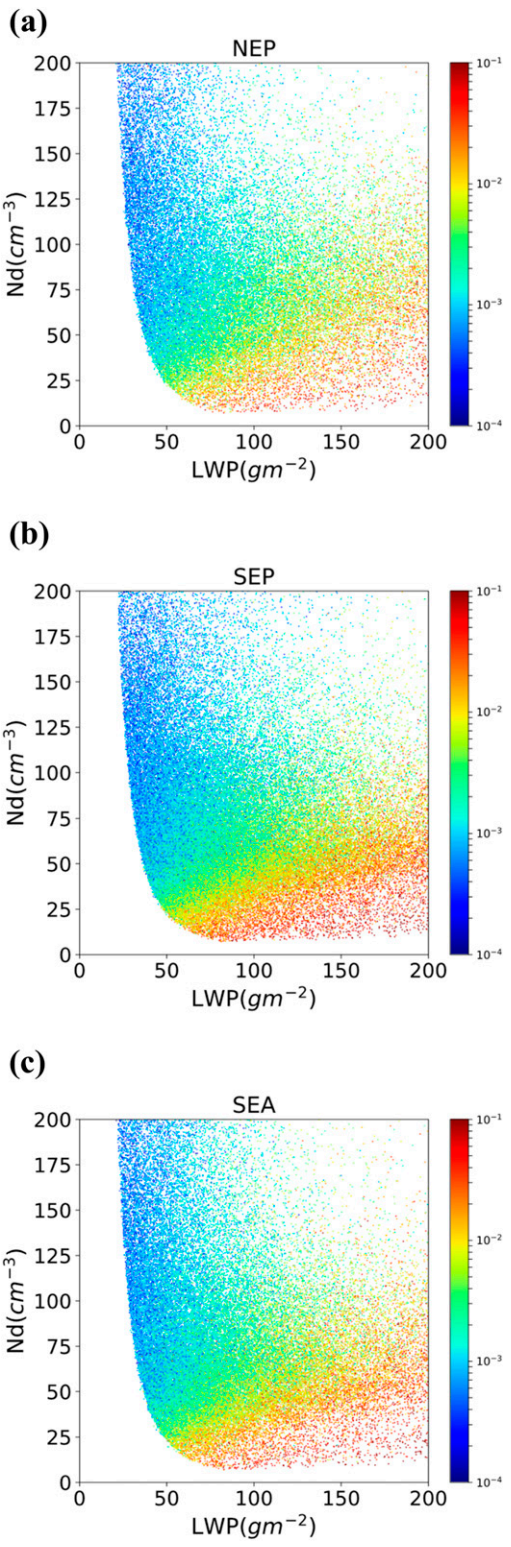

FIG. 9. Scatterplot of R_{cb} (mm h^{-1}) in LWP (g m^{-2})–N_d (cm^{-3}) space for (a) NEP, (b) SEP, and (c) SEA.

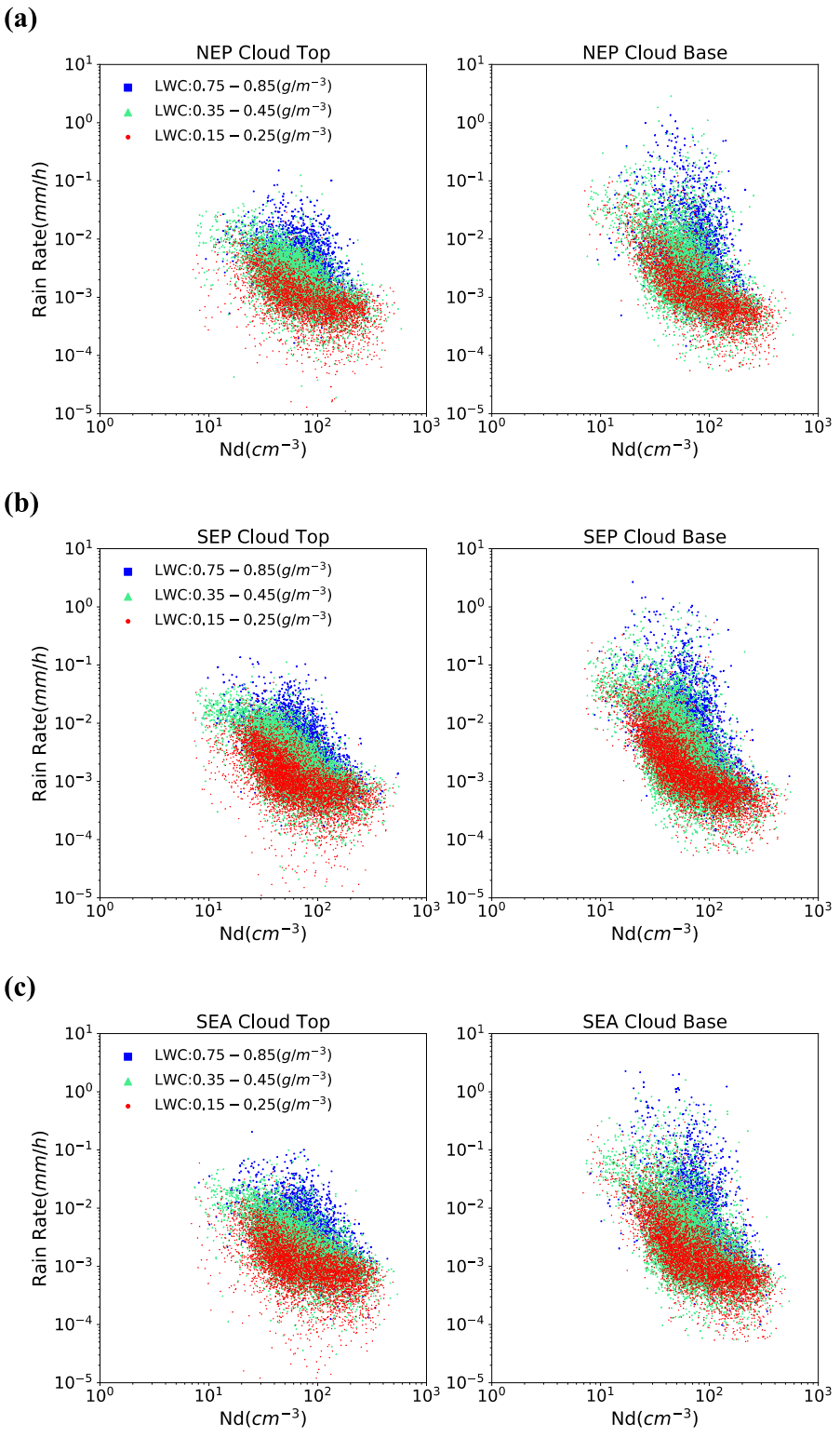

FIG. 10. (left) Cloud-top and (right) cloud-base rain rate as a function of cloud droplet number concentration for different cloud-top liquid water contents for (a) NEP, (b) SEP, and (c) SEA.

water content is calculated from Eq. (8), which assumes a linear increase in liquid water contents with height:

$$\mathrm{LWC} = \frac{2\mathrm{LWP}}{H}. \tag{8}$$

Here, H is the geometrical thickness of cloud in meter. *CloudSat* radar observations contain some intrinsic uncertainty arising from its coarse vertical resolution of about 240 m and its inability to observe cloud-base height below 1 km. The latter can lead to an overestimation of cloud-base height, which will result in higher LWC at cloud top through underestimation of cloud geometrical thickness. It should be noted that the H has some uncertainty inherited from the nature of *CloudSat* observation. There may be ways to accurately estimate the cloud-top liquid water content by combining spaceborne radar and lidar data, but that is left for future work.

The relation between R_{cb} and N_d for all three regions appears to be similar. Regardless of cloud-top liquid water contents, cloud-top rain rate increases with decreasing N_d at cloud top. This is consistent with our physical understanding that autoconversion is enhanced by larger cloud droplets sizes as expressed in Eq. (7). Clouds with N_d of more than 100 cm^{-3} have similar small R_{cb} regardless of cloud-top LWC, from which we infer that raindrop embryo formation through autoconversion rarely occurs in these stratocumulus clouds. The cloud-base rain rate is generally larger than that at cloud top, but there is no significant difference between the top and base for clouds with N_d of more than 100 cm^{-3}. The growth of raindrops through the collection of cloud droplets occurs when significant numbers of raindrop embryos are produced by autoconversion at cloud top, but it seems that these processes are not pronounced in clouds with high N_d where the cloud droplets are too small to produce raindrop embryos through autoconversion. The difference between cloud-top and cloud-base rain rates increases with lower N_d and larger cloud-top LWC, suggesting that collision–coalescence is more efficient in clouds with larger cloud droplets. Figure 11 shows the relation between R_{cb} and N_d as a function of LWP for clouds with similar cloud-top LWC (0.35–0.45 g m^{-3}). For clouds with similar N_d, R_{cb} and its dependency on N_d become stronger as LWP increases. This response of R_{cb} to LWP is consistent with our simplified continuous collection growth model framework discussed in section 3a, which suggests that the accretion growth of raindrops is proportional to LWP. These observational results can be explained by combining a collection growth model with an autoconversion representation as proposed by Khairoutdinov and Kogan (2000, hereafter KK) (see the appendix). Although autoconversion and accretion cannot fully separate (e.g., Shipway and Hill 2012), we inferred that dependency of R_{cb} on N_d from clouds with small cloud-top LWC and LWP can provide information on the upper limit of then dependency of autoconversion rate on N_d.

b. *Response of R_{cb} to N_d*

Figures 12 and 13 show scatterplots and probability density distributions of R_{cb} and N_d for stratocumulus clouds with cloud-top LWC of 0.15–0.25 g $\mathrm{m}^{-3}$and LWP of 40–60 g m^{-3}. These values are chosen so as to obtain robust samples while focusing on clouds with small LWC and LWP. The black solid line indicates the linear regression line obtained from data with cloud droplet number concentration of 30–80 cm^{-3}. Since autoconversion is suppressed in clouds with higher N_d, the

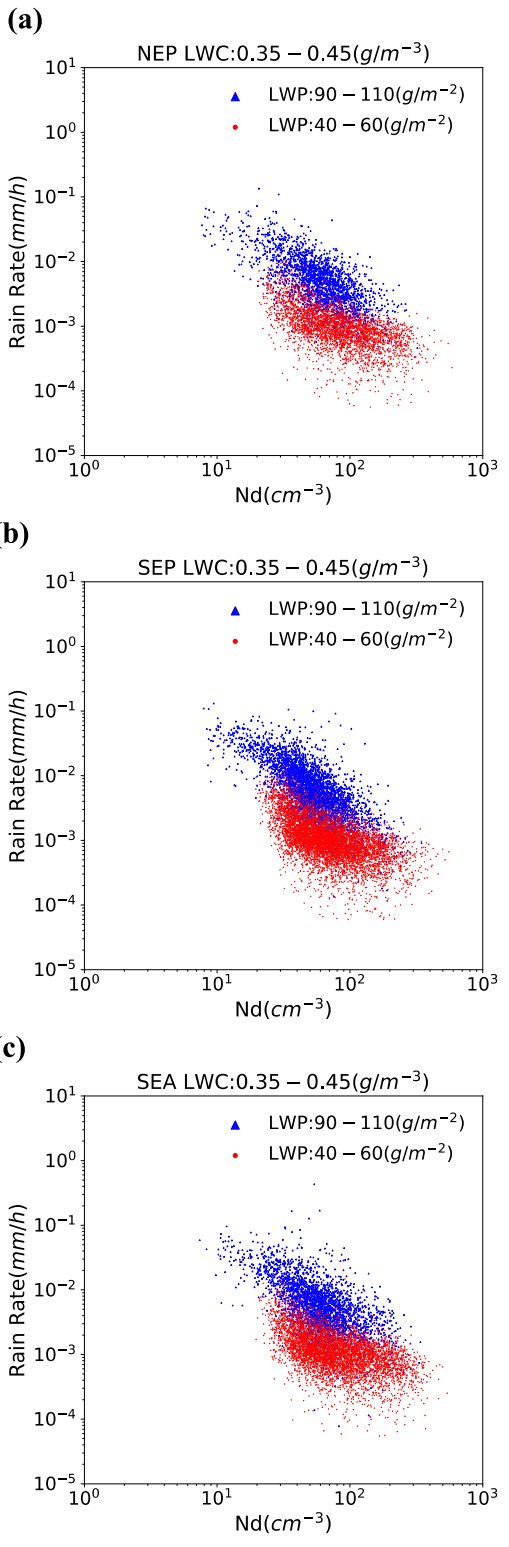

FIG. 11. Relations between cloud-base rain rate and cloud droplet number concentration as a function of LWP for clouds with similar cloud-top LWC (0.35–0.45 g m^{-3}) for (a) NEP, (b) SEP, and (c) SEA.

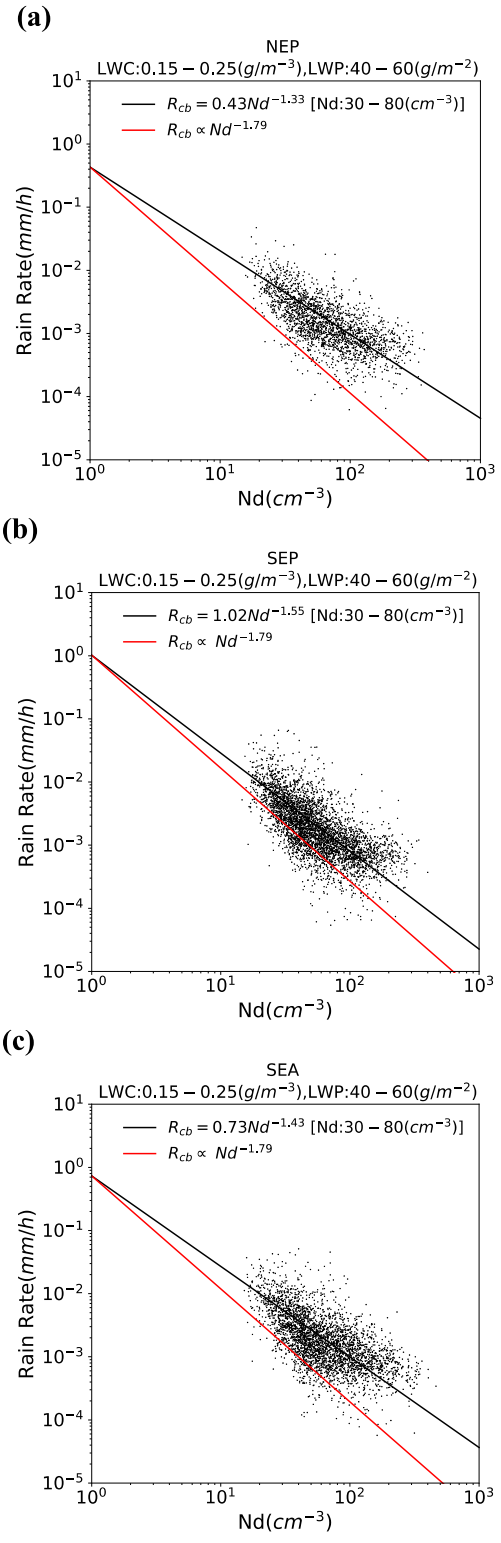

FIG. 12. Scatterplots of cloud-base rain rate and cloud droplet number concentration for (a) NEP, (b) SEP, and (c) SEA. Black solid line indicates the linear regression line obtained from data with cloud droplet number concentration of 30–80 cm^{-3}. The red solid line denotes the dependency of autoconversion rate on cloud droplet number concentration in KK.

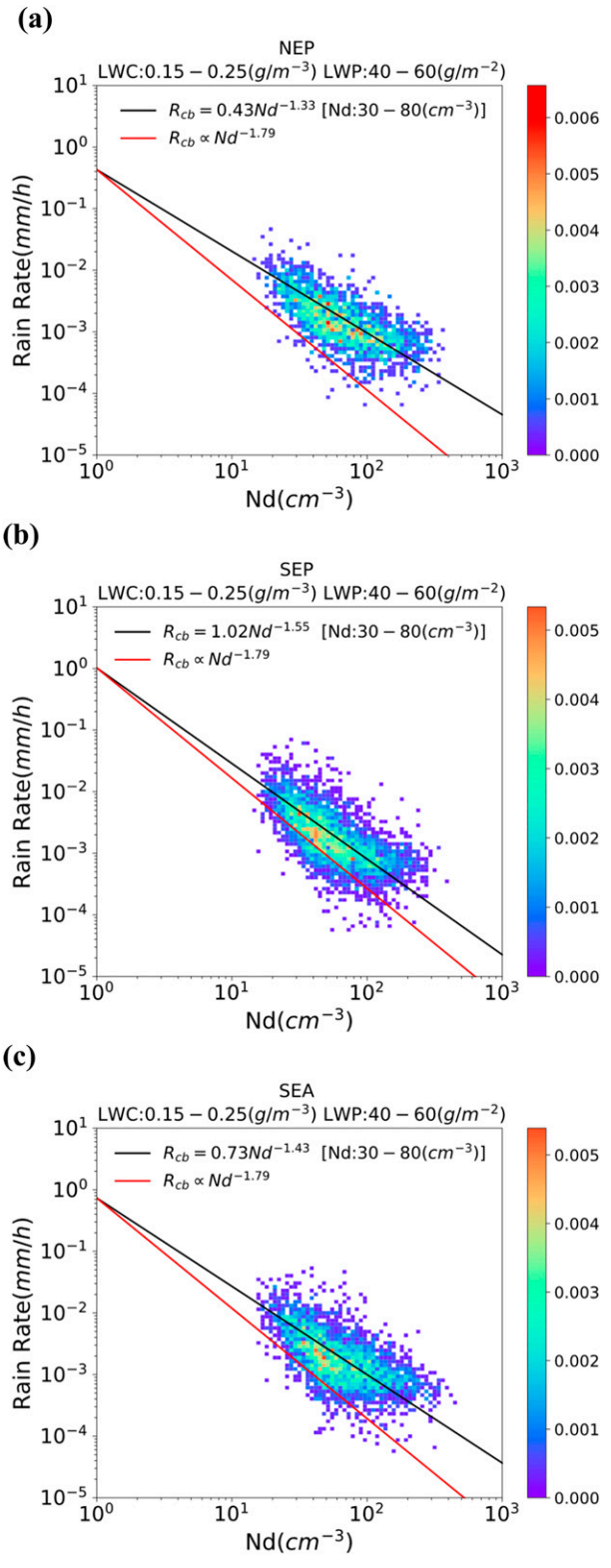

FIG. 13. As in Fig. 11, but for probability density distribution.

inclusion of data with higher N_d could cause an underestimation of the dependency of the autoconversion rate on N_d. The estimated dependency of R_{cb} on N_d is an exponent of −1.328, −1.552, and −1.440 for NEP, SEP, and SEA, respectively. To the best of the authors' knowledge, the range of $-\beta$ in Eq. (7), which corresponds to the estimated dependency, largely varies from −1/3 (Kessler 1969) to −1.79 (KK) depending on the parameterization scheme. The result of this study is closer to that of KK, which is based on LES results in which cloud droplet size distributions for stratocumulus clouds are assumed. Wood (2005b) performed a stochastic collision–coalescence calculation assuming cloud droplet size distributions obtained by in situ aircraft measurements of stratocumulus clouds and found that KK's scheme properly reproduces the autoconversion rate in stratocumulus clouds. The result of this study, obtained using a different approach that cannot fully separate autoconversion with accretion, does nonetheless support the finding of the Wood (2005b) study. Although the dependency of the autoconversion rate on N_d shows some regional variability of about ±0.1, it seems that β is smaller than KK's value of 1.79 within the range of LWP and N_d used in this analysis.

5. Conclusions

In this study, spaceborne observations from A-Train satellites are utilized to obtain statistically robust relations between R_{cb} and the ratio of LWP to N_d (LWP/N_d) for stratocumulus clouds developing in three regions with similar environments, namely, the northeast Pacific off the coast of California, the southeast Pacific off the coast of Peru, and the southeast Atlantic off the coast of Namibia. These regions are selected as they represent areas where strong subsidence associated with the subtropical high is prevalent and plays an integral part in the formation of large decks of stratocumulus clouds.

The relations between R_{cb} and LWP/N_d for all three regions show similar patterns. The cloud-base rain rate R_{cb} is found to be positively correlated with LWP/N_d, which agrees with previous studies. It is also evident from the analysis of the satellite observations that the rate of change of R_{cb} has an increasing trend with larger LWP/N_d. Although previous studies have assumed that this relation is equally applicable for all N_d, the analysis of the large dataset utilized in the present study suggests that this relationship is actually N_d dependent. We found that R_{cb} and its rate of change with respect to LWP/N_d is larger for clouds with lower N_d These characteristics are consistent with our theoretical understanding of 1) autoconversion and the accretion growth of raindrop embryos that become more effective as droplet number concentrations near cloud top become smaller, and 2) that autoconversion is suppressed when the cloud droplet radius is small enough. These results suggest that improving satellite-derived cloud properties through simultaneous utilization of multisatellite sensors will enable us to better understand cloud processes.

Comparing the results of this study with those of Comstock et al. (2004), we found that the changes of R_{cb} with respect to LWP/N_d are nearly the same when LWP/N_d is greater than 1 in both studies. However, the absolute value of R_{cb} in this study is one order of magnitude smaller than that of the Comstock et al. (2004) study. We have shown that this difference can be explained by two reasons. First, a positive bias of the MODIS cloud droplet radius leads to an overestimation of the LWP and an underestimation of cloud droplet number concentration. Second, the physical meaning of the cloud droplet number concentration is different in these two studies. The results of this study represent the number concentrations at cloud top, whereas the Comstock et al. (2004) in situ values represent the cloud-layer-averaged values.

The upper limit of the dependency of autoconversion rate on cloud droplet number concentration [i.e., β in Eq. (7)] is examined by investigating the response of cloud-base and cloud-top rain rates to cloud droplet number concentrations for stratocumulus clouds with smaller cloud-top LWC*s* and LWP*s*. These clouds are chosen because their rain rates are less sensitive to the accretion growth of cloud droplets. It should be noted that autoconversion and accretion cannot be fully separated for these clouds but that using low LWC clouds helps to overcome this difficulty. The value of β is found to be -1.44 ± 0.12 in this study. This result suggests that the dependency of the autoconversion rate in stratocumulus clouds on N_d is greatly underestimated in Kessler type parameterizations that assume $\beta = 1/3$, whereas the parameterization presented by KK in which it is assumed that $\beta = -1.79$, somewhat overestimates the dependency.

Acknowledgments. The *CloudSat* data products were provided by *CloudSat* Data Processing Center at Cooperate Institute for Research in the Atmosphere. We also acknowledge that Y. M. is supported by the Japanese Government Long-term Overseas Fellowship Program.

APPENDIX

Relation between the Slope of log(R_{cb})–log(N_d) Plot and Representation of Autoconversion Parameterization in Bulk Microphysics

The cloud-base rain rate R_{cb} is generally written as Eq. (A1):

$$R_{cb} = \frac{4\pi\rho_w}{3}\int N(r_{drizzle}) r_{drizzle}^3 u(r_{drizzle})\, dr_{drizzle}\,, \qquad \text{(A1)}$$

where $N(r_{drizzle})$, $r_{drizzle}$, and $u(r_{drizzle})$ are the number concentration, radius, and fall velocity of drizzle drops, respectively. As shown in Eq. (7), the autoconversion rate is proportional to $N_d^{-\beta}$ for constant LWC clouds. Assuming that autoconversion produces raindrop embryos of a given size, which is the treatment within the bulk microphysics parameterization proposed by KK, number concentrations of raindrop embryos produced by autoconversion should also be proportional to $N_d^{-\beta}$. As discussed in 3a, accretion growth of raindrops is proportional to the product of cloud-layer-mean collection efficiency and LWP. Assuming that the collection efficiency is independent of cloud droplet size, which is also the treatment within the bulk microphysics parameterization proposed by KK,

raindrop growth by accretion become same for clouds with same LWP. Applying these consideration into Eq. (A1) and denote the drizzle fall speed as $u(R) = aR^b$, the relation among R_{cb}, N_d, and cloud-base raindrop size can be written as Eq. (A2):

$$R_{cb} \propto N_{drizzle} \frac{4\pi}{3} r_{drizzle}^3 a r_{drizzle}^b \propto N_d^{-\beta} a r_{drizzle}^{3+b} . \quad \text{(A2)}$$

Taking the logarithm of both sides of Eq. (A2) gives

$$\log R_{cb} \propto -\beta \log N_d + \text{const}. \quad \text{(A3)}$$

It can be seen from Eq. (A3) that the slope of the logarithm of the R_{cb} as a function of the logarithm of N_d represents the dependency of the autoconversion rate on N_d. Since we assume that collection efficiency is independent of cloud droplet size, it is clear that the collection growth rate is fundamentally a function of total cross-sectional area of collectors (i.e., raindrops), which is modulated by N_d. As N_d becomes smaller, collection growth rate becomes larger through increase of raindrops number concentration. Although collection efficiency is assumed to be independent of cloud droplet size in the above discussion, strictly speaking it is dependent of cloud droplet size. In real data, data with smaller (larger) N_d have a larger (smaller) accretional growth rate and have a stronger (weaker) R_{cb}, which make the slope of log–log plot should be steeper than $-\beta$ of Eq. (A3). Thus, the slope represents the upper limit of dependency of autoconversion on N_d.

REFERENCES

Abel, S. J., D. N. Walters, and G. Allen, 2010: Evaluation of stratocumulus cloud prediction in the Met Office forecast model during VOCALS-REx. *Atmos. Chem. Phys.*, **10**, 10 541–10 559, https://doi.org/10.5194/acp-10-10541-2010.

Ackerman, A. S., O. B. Toon, D. E. Stevens, and J. A. Coakley Jr., 2003: Enhancement of cloud cover and suppression of nocturnal drizzle in stratocumulus polluted by haze. *Geophys. Res. Lett.*, **30**, 1381, https://doi.org/10.1029/2002GL016634.

Albrecht, B. A., 1989: Aerosols, cloud microphysics, and fractional cloudiness. *Science*, **245**, 1227–1230, https://doi.org/10.1126/science.245.4923.1227.

Bennartz, R., 2007: Global assessment of marine boundary layer cloud droplet number concentration from satellite. *J. Geophys. Res.*, **112**, D02201, https://doi.org/10.1029/2006JD007547.

——, and J. Rausch, 2017: Global and regional estimates of warm cloud droplet number concentration based on 13 years of AQUA-MODIS observations. *Atmos. Chem. Phys.*, **17**, 9815–9836, https://doi.org/10.5194/acp-17-9815-2017.

Berry, E. X., and R. L. Reinhardt, 1974: An analysis of cloud drop growth by collection: Part II. Single initial distributions. *J. Atmos. Sci.*, **31**, 1825–1831, https://doi.org/10.1175/1520-0469(1974)031<1825:AAOCDG>2.0.CO;2.

Brenguier, J. L., H. Pawlowska, L. Schuller, R. Preusker, J. Fischer, and Y. Fouquart, 2000: Radiative properties of boundary layer clouds: Droplet effective radius versus number concentration. *J. Atmos. Sci.*, **57**, 803–821, https://doi.org/10.1175/1520-0469(2000)057<0803:RPOBLC>2.0.CO;2.

——, F. Burnet, and O. Geoffroy, 2011: Cloud optical thickness and liquid water path—Does the k coefficient vary with droplet concentration? *Atmos. Chem. Phys.*, **11**, 9771–9786, https://doi.org/10.5194/acp-11-9771-2011.

Bretherton, C. S., T. Uttal, C. W. Fairall, S. E. Yuter, R. A. Weller, D. Baumgardner, and G. B. Raga, 2004: The EPIC 2001 stratocumulus study. *Bull. Amer. Meteor. Soc.*, **85**, 967–978, https://doi.org/10.1175/BAMS-85-7-967.

Comstock, K. K., R. Wood, S. E. Yuter, and C. S. Bretherton, 2004: Reflectivity and rain rate in and below drizzling stratocumulus. *Quart. J. Roy. Meteor. Soc.*, **130**, 2891–2918, https://doi.org/10.1256/qj.03.187.

Feingold, G., and H. Siebert, 2009: Cloud aerosol interactions from the micro to the cloud scale. *Clouds in the Perturbed Climate System: Their Relationship to Energy Balance, Atmospheric Dynamics, and Precipitation*, MIT Press, 319–338.

——, A. McComiskey, D. Rosenfeld, and A. Sorooshian, 2013: On the relationship between cloud contact time and precipitation susceptibility to aerosol. *J. Geophys. Res. Atmos.*, **118**, 10 544–10 554, https://doi.org/10.1002/jgrd.50819.

Geoffroy, O., J. L. Brenguier, and I. Sandu, 2008: Relationship between drizzle rate, liquid water path and droplet concentration at the scale of a stratocumulus cloud system. *Atmos. Chem. Phys.*, **8**, 4641–4654, https://doi.org/10.5194/acp-8-4641-2008.

Grosvenor, D. P., and Coauthors, 2018: Remote sensing of droplet number concentration in warm clouds: A review of the current state of knowledge and perspectives. *Rev. Geophys.*, **56**, 409–453, https://doi.org/10.1029/2017RG000593.

Hansen, J., and L. Travis, 1974: Light scattering in planetary atmospheres. *Space Sci. Rev.*, **16**, 527–610, https://doi.org/10.1007/BF00168069.

Jiang, H., G. Feingold, and A. Sorooshian, 2010: Effect of aerosol on the susceptibility and efficiency of precipitation in warm trade cumulus clouds. *J. Atmos. Sci.*, **67**, 3525–3540, https://doi.org/10.1175/2010JAS3484.1.

Kessler, E., 1969: *On the Distribution and Continuity of Water Substance in Atmospheric Circulations. Meteor. Monogr.*, No. 32, Amer. Meteor. Soc., 84 pp.

Khairoutdinov, M., and Y. Kogan, 2000: A new cloud physics parameterization in a large-eddy simulation model of marine stratocumulus. *Mon. Wea. Rev.*, **128**, 229–243, https://doi.org/10.1175/1520-0493(2000)128<0229:ANCPPI>2.0.CO;2.

King, N. J., and G. Vaughan, 2012: Using passive remote sensing to retrieve the vertical variation of cloud droplet size in marine stratocumulus: An assessment of information content and the potential for improved retrievals from hyperspectral measurements. *J. Geophys. Res.*, **117**, D15206, https://doi.org/10.1029/2012JD017896.

Klein, S. A., and D. L. Hartmann, 1993: The seasonal cycle of low stratiform clouds. *J. Climate*, **6**, 1587–1606, https://doi.org/10.1175/1520-0442(1993)006<1587:TSCOLS>2.0.CO;2.

——, and Coauthors, 2009: Intercomparison of model simulations of mixed-phase clouds observed during the ARM Mixed-Phase Arctic Cloud Experiment. I: Single-layer cloud. *Quart. J. Roy. Meteor. Soc.*, **135**, 979–1002, https://doi.org/10.1002/qj.416.

Kostinski, A. B., 2008: Drizzle rates versus cloud depths for marine stratocumuli. *Environ. Res. Lett.*, **3**, 045019, https://doi.org/10.1088/1748-9326/3/4/045019.

Leon, D. C., Z. Wang, and D. Liu, 2008: Climatology of drizzle in marine boundary layer clouds based on 1 year of data from CloudSat and Cloud-Aerosol Lidar and Infrared Pathfinder Satellite Observations (CALIPSO). *J. Geophys. Res.*, **113**, D00A14, https://doi.org/10.1029/2008JD009835.

Liebe, H. J., T. Manabe, and G. A. Hufford, 1989: Millimeter-wave attenuation and delay rates due to fog/cloud conditions. *IEEE*

Trans. Antennas Propag., **37**, 1617–1623, https://doi.org/10.1109/8.45106.

Mace, G. G., and Q. Zhang, 2014: The CloudSat radar-lidar geometrical profile product (RL-GeoProf): Updates, improvements, and selected results. *J. Geophys. Res. Atmos.*, **119**, 9441–9462, https://doi.org/10.1002/2013JD021374.

Marchand, R., G. G. Mace, T. Ackerman, and G. Stephens, 2008: Hydrometeor detection using *Cloudsat*—An Earth-orbiting 94-GHz cloud radar. *J. Atmos. Oceanic Technol.*, **25**, 519–533, https://doi.org/10.1175/2007JTECHA1006.1.

Martin, G. M., D. W. Johnson, and A. Spice, 1994: The measurement and parameterization of effective radius of droplets in warm stratocumulus clouds. *J. Atmos. Sci.*, **51**, 1823–1842, https://doi.org/10.1175/1520-0469(1994)051<1823:TMAPOE>2.0.CO;2.

Miles, N. L., J. Verlinde, and E. E. Clothiaux, 2000: Cloud droplet size distributions in low-level stratiform clouds. *J. Atmos. Sci.*, **57**, 295–311, https://doi.org/10.1175/1520-0469(2000)057<0295:CDSDIL>2.0.CO;2.

Muhlbauer, A., I. L. McCoy, and R. Wood, 2014: Climatology of stratocumulus cloud morphologies: Microphysical properties and radiative effects. *Atmos. Chem. Phys.*, **14**, 6695–6716, https://doi.org/10.5194/acp-14-6695-2014.

Nelson, K. J., D. B. Mechem, and Y. L. Kogan, 2016: Evaluation of warm-rain microphysical parameterizations in mesoscale simulations of the cloudy marine boundary layer. *Mon. Wea. Rev.*, **144**, 2137–2154, https://doi.org/10.1175/MWR-D-15-0266.1.

Nicholls, S., and J. Leighton, 1986: An observational study of the structure of stratiform cloud sheets: Part I. Structure. *Quart. J. Roy. Meteor. Soc.*, **112**, 431–460, https://doi.org/10.1002/qj.49711247209.

Noble, S. R., and J. G. Hudson, 2015: MODIS comparisons with northeastern Pacific in situ stratocumulus microphysics. *J. Geophys. Res. Atmos.*, **120**, 8332–8344, https://doi.org/10.1002/2014JD022785.

Painemal, D., and P. Zuidema, 2011: Assessment of MODIS cloud effective radius and optical thickness retrievals over the southeast Pacific with VOCALS-REx in situ measurements. *J. Geophys. Res.*, **116**, D24206, https://doi.org/10.1029/2011JD016155.

Parkinson, C. L., 2003: Aqua: An Earth-observing satellite mission to examine water and other climate variables. *IEEE Trans. Geosci. Remote Sens.*, **41**, 173–183, https://doi.org/10.1109/TGRS.2002.808319.

Pawlowska, H., and J.-L. Brenguier, 2003: An observational study of drizzle formation in stratocumulus clouds for general circulation model (GCM) parameterizations. *J. Geophys. Res.*, **108**, 8630, https://doi.org/10.1029/2002JD002679.

Platnick, S., and Coauthors, 2017: The MODIS cloud optical and microphysical products: Collection 6 updates and examples from Terra and Aqua. *IEEE Trans. Geosci. Remote Sens.*, **55**, 502–525, https://doi.org/10.1109/TGRS.2016.2610522.

Raes, F., T. Bates, F. McGovern, and M. van Leide, 2000: The second Aerosol Characterisation Experiment (ACE-2): General overview and main results. *Tellus*, **52B**, 111–125, https://doi.org/10.3402/tellusb.v52i2.16088.

Rogers, R. R., and M. K. Yau, 1989: *A Short Course in Cloud Physics*. 3rd ed. Pergamon Press, 304 pp.

Rossow, W. B., and R. A. Schiffer, 1991: ISCCP cloud data products. *Bull. Amer. Meteor. Soc.*, **72**, 2–20, https://doi.org/10.1175/1520-0477(1991)072<0002:ICDP>2.0.CO;2.

Shipway, B. J., and A. A. Hill, 2012: Diagnosis of systematic differences between multiple parametrizations of warm rain microphysics using a kinematic framework. *Quart. J. Roy. Meteor. Soc.*, **138**, 2196–2211, https://doi.org/10.1002/qj.1913.

Slingo, A., 1990: Sensitivity of the Earth's radiation budget to changes in low clouds. *Nature*, **343**, 49–51, https://doi.org/10.1038/343049a0.

Stephens, G. L., and Coauthors, 2002: The CloudSat mission and the A-Train. *Bull. Amer. Meteor. Soc.*, **83**, 1771–1790, https://doi.org/10.1175/BAMS-83-12-1771.

Stevens, B., and Coauthors, 2003: Dynamics and Chemistry of Marine Stratocumulus—DYCOMS-II. *Bull. Amer. Meteor. Soc.*, **84**, 579–594, https://doi.org/10.1175/BAMS-84-5-579.

Takahashi, H., M. Lebsock, K. Suzuki, G. Stephens, and M. Wang, 2017: An investigation of microphysics and subgrid-scale variability in warm-rain clouds using the A-Train observations and a multiscale modeling framework. *J. Geophys. Res. Atmos.*, **122**, 7493–7504, https://doi.org/10.1002/2016JD026404.

Terai, C. R., R. Wood, D. C. Leon, and P. Zuidema, 2012: Does precipitation susceptibility vary with increasing cloud thickness in marine stratocumulus? *Atmos. Chem. Phys.*, **12**, 4567–4583, https://doi.org/10.5194/acp-12-4567-2012.

Twomey, S., 1959: The nuclei of natural cloud formation part II: The supersaturation in natural clouds and the variation of cloud droplet concentration. *Geofis. Pura Appl.*, **43**, 243–249, https://doi.org/10.1007/BF01993560.

Vali, G., and S. Haimov, 2001: Observed extinction by clouds at 95 GHz. *IEEE Trans. Geosci. Remote Sens.*, **39**, 190–193, https://doi.org/10.1109/36.898682.

vanZanten, M. C., B. Stevens, G. Vali, and D. Lenschow, 2005: Observations of drizzle in nocturnal marine stratocumulus. *J. Atmos. Sci.*, **62**, 88–106, https://doi.org/10.1175/JAS-3355.1.

Wang, H., and G. Feingold, 2009: Modeling mesoscale cellular structures and drizzle in marine stratocumulus. Part I: Impact of drizzle on the formation and evolution of open cells. *J. Atmos. Sci.*, **66**, 3237–3256, https://doi.org/10.1175/2009JAS3022.1.

——, P. J. Rasch, and G. Feingold, 2011: Manipulating marine stratocumulus cloud amount and albedo: A process-modelling study of aerosol-cloud-precipitation interactions in response to injection of cloud condensation nuclei. *Atmos. Chem. Phys.*, **11**, 4237–4249, https://doi.org/10.5194/acp-11-4237-2011.

Winker, D. M., M. A. Vaughan, A. Omar, Y. Hu, K. A. Powell, Z. Liu, W. H. Hunt, and S. A. Young, 2009: Overview of the CALIPSO mission and CALIOP data processing algorithms. *J. Atmos. Oceanic Technol.*, **26**, 2310–2323, https://doi.org/10.1175/2009JTECHA1281.1.

Wood, R., 2005a: Drizzle in stratiform boundary layer clouds. Part I: Vertical and horizontal structure. *J. Atmos. Sci.*, **62**, 3011–3033, https://doi.org/10.1175/JAS3529.1.

——, 2005b: Drizzle in stratiform boundary layer clouds. Part II: Microphysics aspects. *J. Atmos. Sci.*, **62**, 3034–3050, https://doi.org/10.1175/JAS3530.1.

——, 2012: Stratocumulus clouds. *Mon. Wea. Rev.*, **140**, 2373–2423, https://doi.org/10.1175/MWR-D-11-00121.1.